

Chemical Science

Accepted Manuscript



This is an *Accepted Manuscript*, which has been through the Royal Society of Chemistry peer review process and has been accepted for publication.

Accepted Manuscripts are published online shortly after acceptance, before technical editing, formatting and proof reading. Using this free service, authors can make their results available to the community, in citable form, before we publish the edited article. We will replace this *Accepted Manuscript* with the edited and formatted *Advance Article* as soon as it is available.

You can find more information about *Accepted Manuscripts* in the [Information for Authors](#).

Please note that technical editing may introduce minor changes to the text and/or graphics, which may alter content. The journal's standard [Terms & Conditions](#) and the [Ethical guidelines](#) still apply. In no event shall the Royal Society of Chemistry be held responsible for any errors or omissions in this *Accepted Manuscript* or any consequences arising from the use of any information it contains.



www.rsc.org/chemicalscience

Plasmonic Micro-Beads for Fluorescence Enhanced, Multiplexed Protein Detection with Flow Cytometry†

Bo Zhang,^{ac} Jiang Yang,^{ac} Yingping Zou,^{bc} Ming Gong,^a Hui Chen,^a Guosong Hong,^a Alexander L. Antaris,^a Xiaoyang Li,^a Chien-Liang Liu,^a Changxin Chen^a and Hongjie Dai^{*a}

^a Department of Chemistry, Stanford University, Stanford, California 94305, USA. E-mail: hdai@stanford.edu

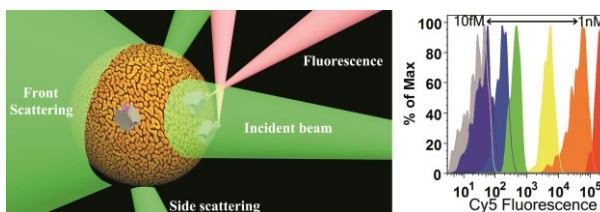
^b College of Chemistry and Chemical Engineering, Central South University, Changsha 410083, China

^c These authors contribute equally to the work.

† Electronic Supplementary Information (ESI) available: Experimental procedures, material characterization data and supporting data reported here. See DOI: 10.1039/b000000x/

Table of contents

Fluorescence enhancement of small molecule fluorophores is achieved on micro-beads through gold nano-island coating, enabling detection of low-abundant protein biomarkers.



Abstract

Micro-bead based multiplexed protein immunoassays have experienced rapid growth in the past decade. Thus far, bead based protein assays have relied on a bulky 240 kDa protein Phycoerythrin (PE) as the reporter dye to afford sufficient detection signal and sensitivity, taking advantage of 25 fluorophores in each protein. Here, we report the synthesis of gold nano-islands coated F beads (4-8 μm) through a two-step seeding-and-growth approach. We developed flow cytometric bead assays with down to 10 fM (~ 0.2 pg/ml) sensitivity by utilizing strong fluorescence enhancement of small molecule fluorophores (Cy-5) on the plasmonic gold beads. By using different fluorescence tags to label gold beads and varying the bead size, we obtained multiplexed plasmonic gold beads for quantification of human cytokine IL-6, IFN-gamma, IL-1 beta, VEGF and an ovarian cancer biomarker CA-125 in biologically relevant media. The low limit of detection surpassed that of glass bead based immunoassays by 2 orders of magnitude, demonstrating the potential of plasmonic gold beads for sensitive protein biomarker quantification.

Introduction

Since the initial introduction in 1977¹, bead based flow cytometric immunoassays have been widely explored for protein analysis. Among various platforms, bead based assay is favorable due to low sample volumes needed, reduced assay processing steps and time, multiplexing capability and the availability of flow cytometry type of instruments²⁻⁴. Currently, bead based assays are widely used for protein (e.g., cytokine) quantification⁵⁻¹², biomarker identification¹³⁻¹⁵ and DNA/microRNA expression profiling for biological research¹⁶⁻²⁰. Cytokines are important signaling molecules regulating hematopoiesis, immune response, cellular activity and are typically expressed over a wide span between sub-pg/ml to thousands of pg/ml²¹. Cytokines at expression levels lower than 1 pg/ml are at the detection limit of various immunoassays and are difficult to measure accurately^{22, 23}. Bead-based flow cytometric assay with enhanced sensitivity could facilitate detecting low abundant proteins, understanding of biological pathways and disease diagnosis at early stages. Cytokine detections could also facilitate assessing responses to therapeutic interventions as those developed for autoimmune diseases⁷.

Since fluorescently conjugated detection molecules are measured on individual beads for signal reporting in a bead based flow cytometric assay, we expect that strategies for amplifying fluorescent emission of fluorophores on each bead could lead to improved sensitivity for flow cytometry based protein analysis. Surface plasmons on metal nanostructures have been found to resonantly couple to fluorophores at excited-state, increasing the radiative decay rate of the excited fluorophores, thus enhancing fluorescence quantum yield²⁴. Indeed, plasmonic gold films on planar substrate have recently been investigated for sensitive molecular analysis in protein microarrays,

utilizing fluorescence enhancement afforded by the underlying plasmonic gold film with plasmon resonance²⁵⁻²⁸. Thus far, most micro-bead based protein assays have relied on using the 240 kDa bulky protein Phycoerythrin (PE) as the reporter. Composed of 25 phycoerythrobilin chromophores, PE molecule is one of the brightest dyes used today due to its large adsorption coefficient and high quantum efficiency²⁹. Current micro-bead based immunoassay affords several pg/ml to sub pg/ml sensitivity for cytokine measurement³⁰. On the other hand, the large protein can cause difficulty in conjugation and steric hindrance effects or background signal issues that are non-ideal for immunoassays³¹. Here, we present for the first time a set of multiplexed plasmonic gold beads for flow cytometric detection of cytokines with high sensitivity using small molecule based fluorophores for reporting.

Results and discussion

Fluorescence enhancement of Cy5 fluorophore by plasmonic gold beads

Plasmonic gold nano-islands coated glass beads (plasmonic gold beads) were prepared through a two-step seeding-and-growth approach³². First, glass beads (8 μm or 4 μm in diameter) were modified with amine groups through reaction with [3-(2-aminoethylamino)propyl]trimethoxysilane (AEPTS). The amine modified glass beads were introduced to a HAuCl_4 solution followed by adding ammonium hydroxide (see experimental section), resulting in $[\text{Au}(\text{OH})_x(\text{NH}_3)_y\text{Cl}_z]_m^{n+}$ clusters attached to the amine modified glass beads. The clusters were reduced to metallic gold nanoparticles (refer to as “gold seeds”) in a sodium borohydride solution. Growth of gold nano-island on the gold seed was performed by introducing the gold seed coated glass beads into a solution

containing HAuCl_4 and NH_2OH , where NH_2OH selectively reduced Au ions onto gold seed. Scanning electron microscopy (SEM) revealed that the glass bead surface was uniformly covered with tortuous gold nano-islands (**Figure 1A and 1B**).

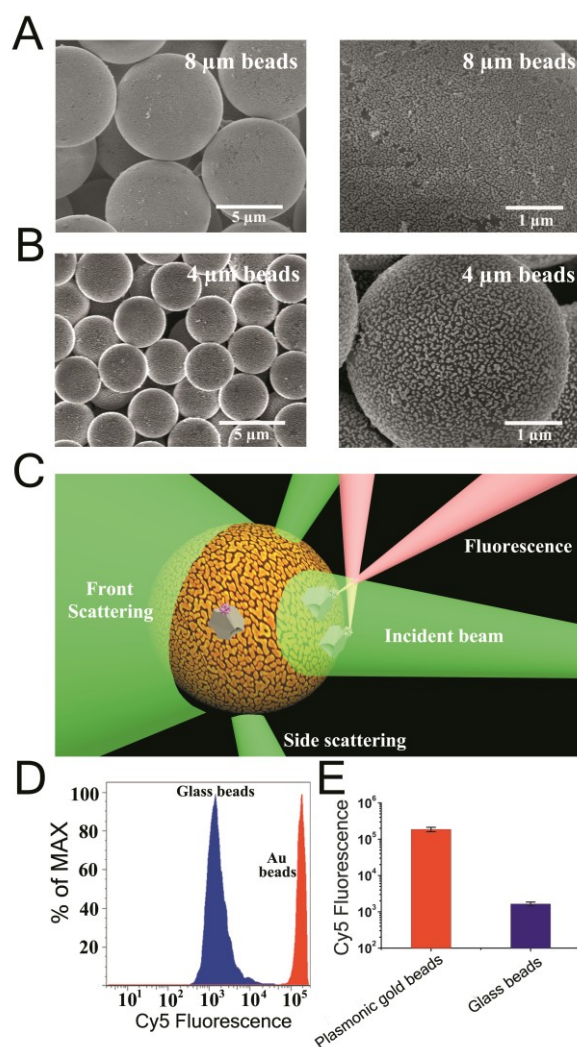


Figure 1. Plasmonic gold nano-island pattern covered glass bead. **A.** Left: A group of 8 micron glass bead uniformly covered with gold nano-islands. Right: A zoom in region of the 8 micron bead showing the details of the gold nano-island pattern on the bead. **B.** Left: A group of 4 micron glass bead uniformly covered with gold nano-islands. Right: A zoom in region of a 4 micron bead showing the details of the gold nano-island pattern on the bead. **C.** A schematic drawing of flow cytometry measurements of a plasmonic gold bead. **D.** Cy5 fluorescence measurement of Cy5-avidin coated plasmonic gold bead and glass bead with flow cytometry, showing the distribution of Cy5 fluorescence intensity on 5,000 plasmonic gold beads and 5,000 glass beads, respectively. **E.** The mean Cy5 fluorescence intensity plot of the 5,000 plasmonic gold beads and 5,000 glass beads, showing vast fluorescence enhancement on plasmonic bead.

We investigated the fluorescence enhancement of gold nano-islands coated beads with various coating morphology by absorbing Cy5-avidin onto the beads via non-specific binding of highly positively charged avidin ($pI = 10.5$) protein with the plasmonic gold bead. Cy5-avidin was also absorbed on glass beads for comparison. The amount of avidin molecules bound to plasmonic gold beads was found to be similar to those bound to glass beads, as manifested by similar enzymatic activity of avidin coated gold/glass bead conjugated with biotinylated horseradish peroxidase (HRP) (**Figure S1**). Therefore, fluorescence enhancement of Cy5 could be reflected by Cy5 fluorescence intensity on plasmonic gold beads versus on glass beads. Cy5 fluorescence intensity on plasmonic gold beads and glass beads under a 640 nm laser excitation were quantified with flow cytometry (**Figure 1C**) as individual beads were passed through a micro fluidic channel. We observed that with low growth concentrations of HAuCl_4 ($< 50 \mu\text{M}$), discrete gold seeds were formed on glass beads, giving low fluorescence enhancement (**Figure S2 and S3**). As the growth concentration increased, the gold seeds increased in size and merged with each other to form gold nano-islands, accompanied by increased Cy5 fluorescence enhancement. At even higher growth concentrations, the gold nano-islands further coalesced to form more continuous gold films, resulting in a significant drop in Cy5 fluorescence suggesting quenching effect (**Figure S2 and S3**).

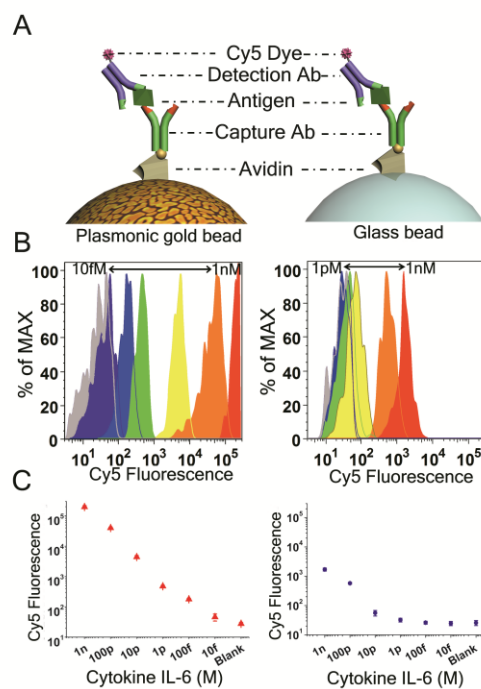
The optimized plasmonic gold beads were covered with gold nano-islands with ~ 100 nm lateral dimensions with gaps between the nano-islands in the 10 - 30 nm range (**Figure 1A and 1B**), affording up to 2 orders of fluorescence enhancement to adsorbed Cy5-avidin molecules over on glass beads (**Figure 1D and 1E**). Appropriate gold nano-island size and gap are important parameters for optimized fluorescence enhancement, as

such structures could enhance local electric fields and afford plasmon-dipole resonance coupling that increases the radiative decay rate of fluorophores in excited state²⁵. Compare to gold nano-island structures on flat substrate with ~ 200 nm lateral dimensions and exhibiting plasmon mode up to long wavelengths (optimal for enhancing fluorophores emitting at 800 nm wavelength²⁵), the 100 nm size gold nano-islands on micro-beads are found to be more efficient in enhancing Cy5 with 670 nm emission peak. The 100 nm gold nano-island size affords a downshift in plasmon modes from the 200 nm ones, giving enhanced resonance coupling with the shorter wavelength emitting cy5 dye than with the IR800 dye^{33, 34}. The lack of long wavelength (800nm) excitation and detection channels for current available flow cytometry systems is another reason why Cy5 was selected as reporter dye rather than IR800 dye.

Single-plexed immunoassays for cytokines

To demonstrate the application of plasmonic gold beads in bead based assays, 8 micron plasmonic gold beads were coated with avidin, followed by attachment of biotinylated capture antibody specific to human cytokine IL-6. The beads were distributed into multiple vials (5,000 beads per vial), and serially diluted human cytokine IL-6 solutions from 1nM to 10 fM plus blank control (each in 100 μ L volume) were added to each vial. After equilibration, washing and detection with fluorophore Cy5 labeled anti human IL-6 antibody (**Figure 2A**), 1,000 beads in each vial were counted by flow cytometry, with Cy5 fluorescence intensity quantified to correlate with the concentration of IL-6 (**Figure 2B**). We observed 5-6 orders of magnitude dynamic range for IL-6 detection, spanning from 1 nM to 10 fM (Figure 2C left graph). The low limit of detection was < 10 fM (< 0.2 pg/mL), which is at least comparable to PE based bead

assays³⁵. Cytokine detection on plasmonic gold beads was reproduced on different days with different batches of beads, and coefficient of variation (CV) of these assays was found to be < 15% for IL-6 concentrations over 100 fM and < 30% for concentrations below 100 fM (**Table S1**). Identical immunoassays were also performed on glass beads (Figure 2C right graph), affording detection limit at 1 pM (20 pg/mL), which was inferior to assays performed with gold beads (**Figure 2**). This sensitivity difference was consistent with protein detection on flat plasmonic gold substrate versus glass substrate^{25, 26}. With 4 μm plasmonic gold beads, we also observed high fluorescence enhancement of Cy5 over glass beads and 10 fM sensitivity for human IL-6 quantification (**Figure S4**).



Multiplexed cytokine immunoassays using encoded plasmonic gold beads

Previously, multiplexed polymer beads for immunoassays have been made by differentiating beads by size³⁶, or by the different ratios of two fluorophore tags conjugated onto the beads³⁷. For demonstration of multiplexed plasmonic gold beads, we combined bead size differentiation with different fluorophore tags. Micro-beads of various sizes can be differentiated by the degree of front scattering (proportional to bead diameter) of an incident laser beam in flow cytometry³⁸. A given size bead could be further divided into several sub-groups based on different fluorescence tags on beads. Different beads could then each be conjugated to antibody against a specific protein of interest, thus affording a set of multiplexed bead system for quantification of multiple protein biomarkers. For proof of concept, we used antibody immobilized 4 and 8 micron plasmonic gold beads with or without Cy3 or Alexa Fluor 488 tagging for constructing a set of 6-plexed beads for simultaneous quantification of human cytokines and a human ovarian cancer biomarker CA-125 (**Figure 3A**). Light scattering plot (side scatter versus front scatter) clearly revealed two different regions of beads, corresponding to 4 micron beads and 8 micron beads respectively (**Figure 3B** upper left graph). The 4 micron beads and 8 micron beads were further differentiated into 3 sub regions based on the Cy3 and Alexa 488 fluorescence intensities (**Figure 3B** upper right graph and lower left graph), which was also revealed by confocal fluorescence imaging (**Figure 3B** lower right graph). This result confirmed the feasibility of plasmonic gold beads multiplexing, as the size of beads can be determined by front scattering, and the fluorescence tagging of the bead can be detected by specific laser/filter set in the flow cytometry system.

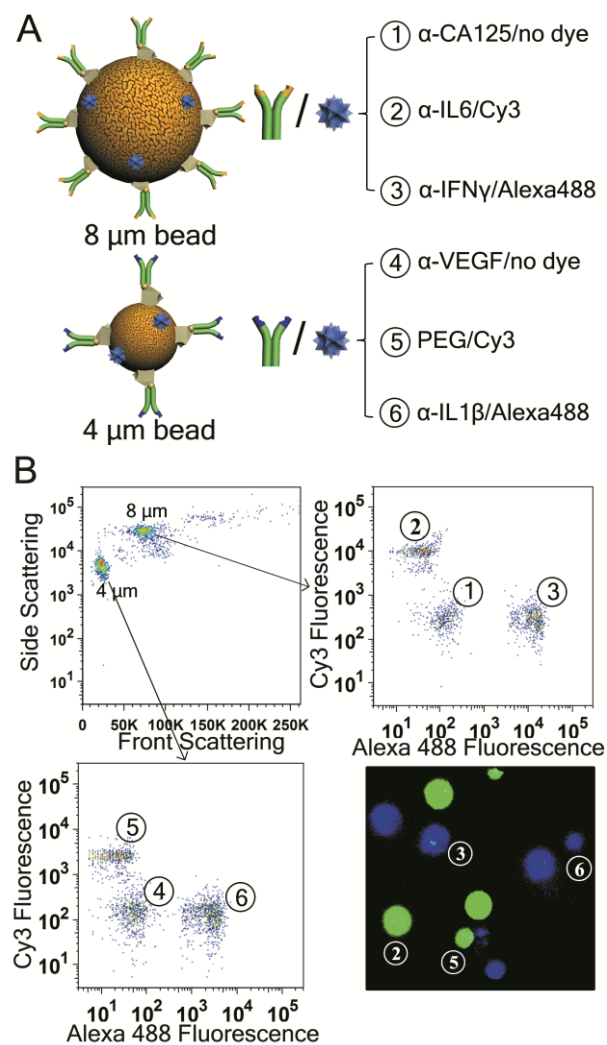


Figure 3. Coding plasmonic gold beads for multiplexed biomarker measurement **A.** Design scheme of a plasmonic bead system for 6-plexed biomarker measurement; 8 micron beads were labeled with anti human CA-125 capture antibody; 8 micron alexa fluor 488 coded bead was labeled with anti human IFN-gamma capture antibody; and 8 micron Cy3 coded bead was labeled with anti human IL-6 capture antibody. 4 micron bead was labeled with anti human VEGF capture antibody; 4 micron alexa fluor 488 coded bead was labeled with anti IL-1 beta capture antibody; 4 micron Cy3 coded bead was labeled with PEG as negative control. **B.** Flow cytometry measurement of a mixture of the beads in **A.** 4 micron and 8 micron bead are resolved from side-scattering versus front-scattering plot (top left). In each bead sized region, 3 sub-regions can be resolved from Cy3 fluorescence versus alexa fluor 488 fluorescence plots, which are Cy3 coded bead, alexa 488 coded beads, and non-coding bead. Bottom right: Confocal fluorescence mapping of the 6-plexed bead system prior to being used for biomarker sensing: green color reflects Cy3 fluorescence; blue color reflects alexa 488 fluorescence. Bead 1 and 4 are not resolved due to the lack of any fluorescence coding.

The dynamic range and sensitivity of our multiplexed gold beads were assessed through calibrating serial dilutions of a CA-125, IL-6, IFN-gamma, VEGF and IL-1 beta protein mixture to different concentrations. After probing with the protein mixture, a mixture of Cy5 conjugated detection antibodies, each specific to one biomarker, was introduced to plasmonic gold beads solution for labeling biomarkers on each bead with Cy5 dye (**Figure 4A**). Up to 5-6 orders (though not for VEGF likely due to lower antibody affinity) of dynamic range were achieved for multiplexed detection of cytokines (**Figure 4B and Figure S5**). Sub-pg/ml (10 fM) cytokine sensitivity was achieved and CA-125 was detectable down to 0.12 U/ml. Note that through careful selection of antibody pairs (from different vendors) for cytokine detection to reduce cross-reactivity, we were able to eliminate matrix effect for cytokine detection, as cytokine calibration curve plotted from multiplexed detection behaves similar to that plotted from single-plex detection (**Figure 2C and 4B**). Specificity of multiplexed protein detection was confirmed through detection of individual types of proteins one at a time with the 6-plex plasmonic gold bead system (**Figure 4B and Figure S6**).

Perhaps one of the most important features of bead based immunoassay is its capability for multiplexing, which has been realized through two approaches previously: utilizing multiple sizes of micro-beads for quantification of different analytes³⁹ and tagging different fluorophores onto micro-beads of the same size^{37, 40}. We combined the two approaches to afford multiplexing capability of gold plasmonic bead based immunoassays. There are more choices of visible dyes with non-overlapping emission spectra for tagging plasmonic beads when red dye Cy5 was introduced for signal

reporting, which could lead to much higher degree of multiplexing than demonstrated in the current work.

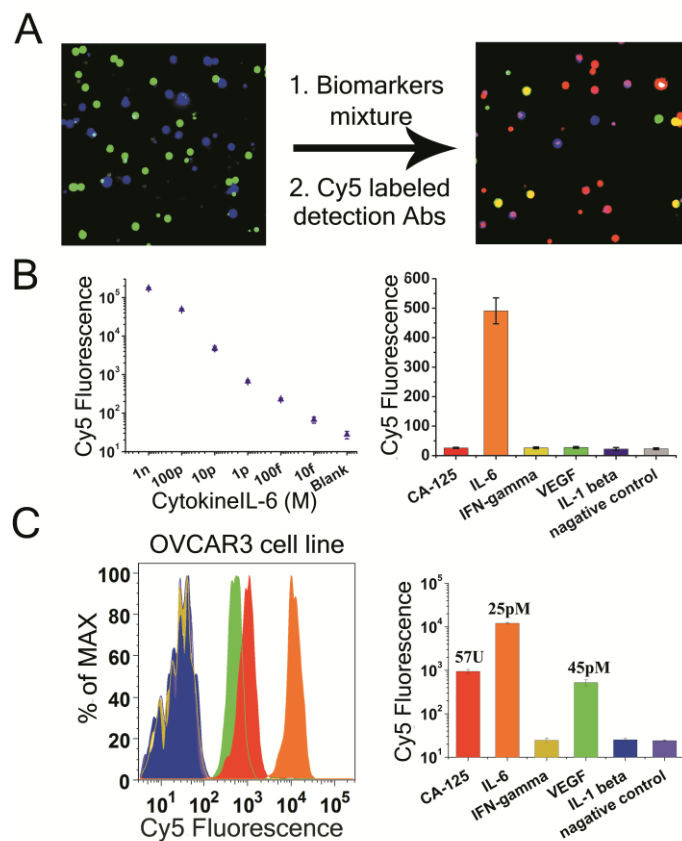


Figure 4. Multiplexed biomarker quantification with fM sensitivity. **A.** Confocal fluorescence mapping/imaging of the 6-plexed bead system before and after biomarker detection in a mixture of CA-125, IFN-gamma, IL-6, VEGF and IL-1 beta each at 100 pM: red color reflects Cy5 fluorescence; yellow reflects the co-localization of Cy5 and Cy3; purple reflects the co-localization of Cy5 and Alexa fluor 488. **B.** Left: Fluorescence quantification data for a serially diluted IL-6 antigen solution by our 6-plexed bead system. Right: Bar graph for selectivity test of the multiplexed plasmonic bead assay, reflecting Cy5 fluorescence on each of the 6 sub-region of plasmonic gold beads where 1pM IL-6 (middle) was applied for biomarker quantification with the multiplexed plasmonic beads system. **C.** Left: Protein detection result in ovarian cancer cell line OVCAR3 culture medium: IL-6 (orange), CA-125 (red) and VEGF (green) were identified. Right: Quantification of protein concentrations in the cell culture medium of OVCAR3 cell line by fitting Cy5 mean fluorescence into the calibration curve of each protein.

Multiplex detection of cytokines and cancer markers from cell culture media

To demonstrate the capability of our multiplexed plasmonic bead system for protein quantification in biological samples, we performed cytokine and CA125 detection in cancer cell culture medium through flow cytometric immunoassay on plasmonic gold beads. Human ovarian cancer cell lines OVCAR3 and SKOV3 were cultured for 48 h and their culture media were collected for cytokine and CA125 measurements (**Figure 4C and Figure S7**). OVCAR3 is an ovarian cancer cell line known to secrete CA125 while SKOV3 is a CA125 negative ovarian cancer cell line⁴¹. We detected high CA-125, IL-6 and VEGF expression levels in the OVCAR3 culture medium (**Figure 4C**), and IL-6 and VEGF in the SKOV3 culture medium (**Figure S7**). Linear regression of blank corrected calibration curve was performed for each cytokine and concentration of each analyte in cell lysate was determined by fitting Cy5 fluorescence signal into the corresponding curve (**Figure 4B and Figure S5**). 25 (+/- 1.2) pM of IL-6, 45 pM (+/- 5.6) of VEGF and 57 (+/- 6.2) U/ml of CA-125 were detected in the OVCAR3 culture medium (**Figure 4C**), while 42 pM (+/- 2.1) IL-6 and 54 pM (+/- 7.8) VEGF was observed the in SKOV3 culture medium (**Figure S7**). Cytokine concentration value below the lower limit of detection was considered as undetectable and was not computed. We conducted Enzyme Linked Immunosorbent assay (ELISA) measurement of IL-6 in cell culture media to validate the plasmonic micro-bead data. 29 (+/- 3.5) pM IL-6 in OVCAR3 culture media and 42 (+/- 6.3) pM IL-6 in SKOV3 culture media were detected by ELISA (**Figure S8**), which was highly consistent with IL-6 level measured by plasmonic micro-bead assay.

A panel of biomarkers, rather than single-analyte measurements, is likely to improve the sensitivity and specificity in cancer detection, staging and monitoring⁴²⁻⁴⁴.

Simultaneous detection of clinically used low-specificity cancer biomarkers and additional inflammatory cytokines and chemokines could lead to protein profiling of various cancer types, allowing for cancer diagnosis at early stage^{45, 46}. The wide dynamic range of our assay enables bead based quantification of a panel of biomarkers with a wide concentration distribution from sub-pg/ml to tens of ng/ml. Our plasmonic micro-bead assay was able to detect cytokine VEGF and IL-6 from cancer cell culture media, which are potent stimulating factors for angiogenesis and can promote tumor formation^{47, 48}.

Conclusion

In conclusion, fluorescence enhancement of small fluorophores is achieved on micro-beads through coating of Au nanostructures on glass micro-beads. The fluorescence enhancement effect facilitates bead based immunoassay using small molecule reporters as an alternative to PE, enhancing the ability of measuring low abundant protein biomarkers such as cytokines at concentrations near the lower limit of detection of existing methods. Multiplexed plasmonic beads have been demonstrated and can be expanded. The plasmonic gold beads may have high potential for research and clinical usage for biomarker development and early stage disease detection.

Acknowledgements

This work is supported by the Stanford SPARK program. B. Z. acknowledges support from the Stanford Bio-X SIGF fellowship. We thank David R. Parks and Cathy Crumpton for their help in FACS operation at Stanford Shared FACS Facility.

Notes and References

1. P. K. Horan and L. L. Wheelless, Jr., *Science*, 1977, 198, 149-157.
2. V. V. Krishhan, I. H. Khan and P. A. Luciw, *Crit Rev Biotechnol*, 2009, 29, 29-43.
3. R. J. Fulton, R. L. McDade, P. L. Smith, L. J. Kienker and J. R. Kettman, Jr., *Clinical chemistry*, 1997, 43, 1749-1756.
4. I. V. Jani, G. Janossy, D. W. Brown and F. Mandy, *Lancet Infect Dis*, 2002, 2, 243-250.
5. T. B. Martins, B. M. Pasi, J. W. Pickering, T. D. Jaskowski, C. M. Litwin and H. R. Hill, *Am J Clin Pathol*, 2002, 118, 346-353.
6. J. F. D. Siawaya, T. Roberts, C. Babb, G. Black, H. J. Golakai, K. Stanley, N. B. Bapela, E. Hoal, S. Parida, P. van Helden and G. Walzl, *PLoS one*, 2008, 3, e2535.
7. S. M. Churchman, J. Geiler, R. Parmar, E. A. Horner, L. D. Church, P. Emery, M. H. Buch, M. F. McDermott and F. Ponchel, *Clinical and experimental rheumatology*, 2012, 30, 534-542.
8. E. Morgan, R. Varro, H. Sepulveda, J. A. Ember, J. Apgar, J. Wilson, L. Lowe, R. Chen, L. Shivraj, A. Agadir, R. Campos, D. Ernst and A. Gaur, *Clin Immunol*, 2004, 110, 252-266.
9. E. B. Cook, J. L. Stahl, L. Lowe, R. Chen, E. Morgan, J. Wilson, R. Varro, A. Chan, F. M. Graziano and N. P. Barney, *Journal of immunological methods*, 2001, 254, 109-118.
10. M. G. D. J. Liebertz and A. L. Epstein, *J Immunol*, 2010, 185, 5668-5668.
11. E. W. Newell, N. Sigal, S. C. Bendall, G. P. Nolan and M. M. Davis, *Immunity*, 2012, 36, 142-152.
12. U. Sester, M. Fousse, J. Dirks, U. Mack, A. Prasse, M. Singh, A. Lalvani and M. Sester, *PLoS one*, 2011, 6, e17813.
13. J. Du, P. Bernasconi, K. R. Clauser, D. R. Mani, S. P. Finn, R. Beroukhim, M. Burns, B. Julian, X. P. Peng, H. Hieronymus, R. L. Maglathlin, T. A. Lewis, L. M. Liao, P. Nghiemphu, I. K. Mellinshoff, D. N. Louis, M. Loda, S. A. Carr, A. L. Kung and T. R. Golub, *Nature biotechnology*, 2009, 27, 77-83.
14. J. Ling, U. Wiederkehr, S. Cabiness, K. R. Shroyer and J. P. Robinson, *Diagn Cytopathol*, 2008, 36, 76-84.
15. L. A. Sklar, M. B. Carter and B. S. Edwards, *Curr Opin Pharmacol*, 2007, 7, 527-534.
16. J. Lu, G. Getz, E. A. Miska, E. Alvarez-Saavedra, J. Lamb, D. Peck, A. Sweet-Cordero, B. L. Ebert, R. H. Mak, A. A. Ferrando, J. R. Downing, T. Jacks, H. R. Horvitz and T. R. Golub, *Nature*, 2005, 435, 834-838.
17. M. P. Hunter, N. Ismail, X. L. Zhang, B. D. Aguda, E. J. Lee, L. B. Yu, T. Xiao, J. Schafer, M. L. T. Lee, T. D. Schmittgen, S. P. Nana-Sinkam, D. Jarjoura and C. B. Marsh, *PLoS one*, 2008, 3, e3694.
18. Y. Shimono, M. Zabala, R. W. Cho, N. Lobo, P. Dalerba, D. L. Qian, M. Diehn, H. P. Liu, S. P. Panula, E. Chiao, F. M. Dirbas, G. Somlo, R. A. R. Pera, K. Q. Lao and M. F. Clarke, *Cell*, 2009, 138, 592-603.
19. G. A. Calin and C. M. Croce, *Nat Rev Cancer*, 2006, 6, 857-866.
20. Y. L. Gao, W. L. Stanford and W. C. W. Chan, *Small*, 2011, 7, 137-146.
21. T. J. Kindt, R. A. Goldsby, B. A. Osborne and J. Kuby, *Kuby immunology*, W.H. Freeman, New York, 6th edn., 2007.
22. G. Kleiner, A. Marcuzzi, V. Zanin, L. Monasta and G. Zauli, *Mediators of inflammation*, 2013, 2013, 434010.
23. F. Chowdhury, A. Williams and P. Johnson, *J Immunol Methods*, 2009, 340, 55-64.
24. K. Aslan, I. Gryczynski, J. Malicka, E. Matveeva, J. R. Lakowicz and C. D. Geddes, *Current opinion in biotechnology*, 2005, 16, 55-62.

25. S. M. Tabakman, L. Lau, J. T. Robinson, J. Price, S. P. Sherlock, H. Wang, B. Zhang, Z. Chen, S. Tangsombatvisit, J. A. Jarrell, P. J. Utz and H. Dai, *Nature communications*, 2011, 2, 466.
26. B. Zhang, J. Price, G. S. Hong, S. M. Tabakman, H. L. Wang, J. A. Jarrell, J. Feng, P. J. Utz and H. J. Dai, *Nano Res*, 2013, 6, 113-120.
27. B. Zhang, J. A. Jarrell, J. V. Price, S. M. Tabakman, Y. G. Li, M. Gong, G. S. Hong, J. Feng, P. J. Utz and H. J. Dai, *Plos One*, 2013, 8, e71043.
28. F. Xie, J. S. Pang, A. Centeno, M. P. Ryan, D. J. Riley and N. M. Alford, *Nano Res*, 2013, 6, 496-510.
29. E. Dagnolo, R. Rizzo, S. Paoletti and E. Murano, *Phytochemistry*, 1994, 35, 693-696.
30. <http://www.rndsystems.com/Products/LHSC000>
31. <http://www.piercenet.com/method/overview-detection-probes>
32. S. M. Tabakman, Z. Chen, H. S. Casalongue, H. Wang and H. Dai, *Small*, 2011, 7, 499-505.
33. K. Aslan, I. Gryczynski, J. Malicka, E. Matveeva, J. R. Lakowicz and C. D. Geddes, *Curr Opin Biotech*, 2005, 16, 55-62.
34. J. R. Lakowicz, *Analytical biochemistry*, 2005, 337, 171-194.
35. Lumindex xMap technology. <http://www.millipore.com/bmia/flx4/multiplexing-instruments#tab1=2>
36. T. M. McHugh, R. C. Miner, L. H. Logan and D. P. Stites, *Journal of clinical microbiology*, 1988, 26, 1957-1961.
37. M. F. Elshal and J. P. McCoy, *Methods*, 2006, 38, 317-323.
38. H. B. Steen, *Cytometry*, 1980, 1, 26-31.
39. M. Hartmann, J. Roeraade, D. Stoll, M. F. Templin and T. O. Joos, *Anal Bioanal Chem*, 2009, 393, 1407-1416.
40. K. Braeckmans, S. C. De Smedt, M. Leblans, R. Pauwels and J. Demeester, *Nat Rev Drug Discov*, 2002, 1, 447-456.
41. M. Boivin, D. Lane, A. Piche and C. Rancourt, *Gynecologic oncology*, 2009, 115, 407-413.
42. R. P. Huang, B. Burkholder, V. S. Jones, W. D. Jiang, Y. Q. Mao, Q. L. Chen and Z. Shi, *Curr Proteomics*, 2012, 9, 55-70.
43. S. M. Hanash, S. J. Pitteri and V. M. Faca, *Nature*, 2008, 452, 571-579.
44. V. Kulasingam and E. P. Diamandis, *Nat Clin Pract Oncol*, 2008, 5, 588-599.
45. Z. Zhang, R. C. Bast, Jr., Y. Yu, J. Li, L. J. Sokoll, A. J. Rai, J. M. Rosenzweig, B. Cameron, Y. Y. Wang, X. Y. Meng, A. Berchuck, C. Van Haaften-Day, N. F. Hacker, H. W. de Bruijn, A. G. van der Zee, I. J. Jacobs, E. T. Fung and D. W. Chan, *Cancer Res*, 2004, 64, 5882-5890.
46. G. Mor, I. Visintin, Y. Lai, H. Zhao, P. Schwartz, T. Rutherford, L. Yue, P. Bray-Ward and D. C. Ward, *Proc Natl Acad Sci U S A*, 2005, 102, 7677-7682.
47. P. Carmeliet, *Nature*, 2005, 438, 932-936.
48. M. Karin, *Nature*, 2006, 441, 431-436.